NEW: Network-Enabled Electronic Warfare for Target Recognition

QILIAN LIANG
University of Texas at Arlington

XIUZHEN CHENG
George Washington University

SHERWOOD W. SAMN
Air Force Research Laboratory

Network-enabled electronic warfare (NEW) is the development of modeling and simulation efforts that explore the advantages and limitations of NEW concepts. The advantages of linking multiple electronic support measures (ESM) and electronic attack (EA) assets to achieve improved capabilities across a networked battle force have yet to be quantified. In this paper, we utilize radar sensors as ESM and EA assets to demonstrate the advantages of NEW in collaborative automatic target recognition (CATR). Signal (waveform) design for radar sensor networks (RSN) in NEW is studied theoretically. The conditions for waveform coexistence and the interferences among waveforms in RSN are analyzed. We apply the NEW to CATR via waveform diversity combining and propose maximum-likelihood (ML)-ATR algorithms for nonfluctuating targets as well as fluctuating targets. Simulation results indicate that our NEW-CATR performs much better than the single sensor-based ATR algorithm for nonfluctuating and fluctuating targets.

I. INTRODUCTION AND MOTIVATION

In current and future military operational environments such as the Global War on Terrorism (GWOT) and Maritime Domain Awareness (MDA), war fighters require technology that can support their information needs in a manner that is independent of their location and consistent with their level of command or responsibility and operational situation. To support this need, the U.S. Department of Defense (DoD) has developed the concept of network centric warfare (NCW) defined as "*military operations that exploit state-of-the-art information and networking technology to integrate widely dispersed human decision makers, situational and targeting sensors, and forces and weapons into a highly adaptive, comprehensive system to achieve unprecedented mission effectiveness*" [1]. Network-enabled electronic warfare (NEW) is the form of electronic combat used in NCW. Focus is placed on a network of interconnected, adapting systems that are capable of making choices about how to survive and achieve their design goals in a dynamic environment. The goal of NEW is to develop modeling and simulation efforts that explore the advantages and limitations of NEW concepts. The advantages of linking multiple electronic support measures (ESM) and electronic attack (EA) assets to achieve improved capabilities across a networked battle force have yet to be quantified [2]. In this paper we utilize radar sensors as ESM and EA assets to demonstrate the advantages of NEW in collaborative automatic target recognition (CATR). The network of radar sensors should operate with multiple goals managed by an intelligent platform network that can manage the dynamics of each radar to meet the common goals of the platform rather than each radar operating as an independent system. Therefore, it is significant to perform signal design and processing and networking cooperatively within and between platforms of radar sensors and their communication modules. This need is also apparent in the recent solicitations from the U.S. Office of Naval Research [2, 3]. For example, in [3] it is stated, "Algorithms are sought for fused and/or coherent cross-platform RF sensing. The focus of this effort is to improve surveillance utilizing a network, not fusion of disparate sensor products. The algorithms should be capable of utilizing RF returns from multiple aspects in a time-coordinated sensor network."

In this paper, we study waveform design and diversity algorithms for radar sensor networks. Waveform diversity is the technology that allows one or more sensors onboard a platform to automatically change operating parameters, e.g., frequency, gain pattern, and pulse repetition frequency (PRF), to meet the varying environments. It has long been recognized that judicious use of properly designed waveforms, coupled with advanced receiver strategies,

is fundamental to fully utilizing the capacity of the electromagnetic spectrum. However, it is the relatively recent advances in hardware technology that are enabling a much wider range of design freedoms to be explored. As a result there are emerging and compelling changes in system requirements such as more efficient spectrum usage, higher sensitivities, greater information content, improved robustness to errors, reduced interference emissions, etc. The combination of these changes is fueling a worldwide interest in the subject of waveform design and the use of waveform diversity techniques.

Most existing works on waveform design and selection are focused on the single radar or sonar system. In 1974 Fitzgerald [8] demonstrated the inappropriateness of selection of waveforms based on measurement quality alone: the interaction between the measurement and the track can be indirect, but must be accounted for. Since then, extensive works on waveform design have been reported. Bell [6] used information theory to design radar waveforms for the measurement of extended radar targets exhibiting resonance phenomena. In [5], the singularity expansion method was used to design discriminant waveforms such as K-pulse, E-pulse, and S-pulse. Sowelam and Tewfik [23] developed a signal selection strategy for radar target classification, and a sequential classification procedure was proposed to minimize the average number of necessary signal transmissions. Intelligent waveform selection was studied in [4, 12], but the effect of Doppler shift was not considered. In [16], time-frequency–based generalized chirps were used as waveform for detection and estimation. In [15], the performance of constant frequency (CF) and linear frequency modulated (LFM) waveform fusion from the standpoint of the whole system was studied, but the effect of clutter was not considered. In [24], a new time-frequency signal decomposition algorithm based on the S-method was proposed and evaluated on the high-frequency surface-wave radar (HFSWR) data; it demonstrated that it provided an effective way for analyzing and detecting maneuvering air targets with significant velocity changes, including target signal separation from the heavy clutter. In [25], CF and LFM waveforms were studied for a sonar system, but it was assumed that the sensor was nonintelligent (i.e., the waveform cannot be selected adaptively). All the above studies and design methods focused on the waveform design or selection for a single active radar or sonar system. In [21], cross-correlation properties of two radars are briefly mentioned, and the binary coded pulses using simulated annealing [7] are highlighted. However, the cross-correlation of two binary sequences such as binary coded pulses (e.g., Barker sequence) is much easier to study than that of two analog radar waveforms.

In this paper, we focus on the waveform diversity and design for radar sensor networks using the CF pulse waveform. Compared with previous works, this paper has the following novelties.

1) Our focus is placed on a network of interconnected, adapting radar systems that are capable of making choices about how to survive and achieve their design goals in a dynamic environment.

2) We study waveform design and diversity for radar sensors networks. In space-time adaptive processing (STAP) [18], the waveform (pulse) design is essentially for a single radar system. The pulse is sent repeatedly at different times, and the echos are received and processed by an antenna array, and no interference exists among pulses if the pulse repetition interval is large enough.

3) We investigate CATR using radar sensor networks and compare it against the single-radar system in CATR.

4) Simulations are performed for nonfluctuating targets as well as fluctuating targets, and a real-world application example, sense-through-foliage target detection, is presented.

The rest of this paper is organized as follows: In Section II, we study the coexistence of radar waveforms. In Section III, we analyze the interferences among radar waveforms. In Section IV, we propose a RAKE structure for waveform diversity combining and present a maximum-likelihood (ML) algorithm for CATR. In Section V, we provide simulation results on ML-CATR. In Section VI, we conclude this paper and discuss future research.

II. COEXISTENCE OF RADAR WAVEFORMS

In radar sensor networks (RSN), radar sensors interfere with each other, and the signal-to-interference-ratio may be very low if the waveforms are not properly designed. In this paper, we introduce orthogonality as one criterion for waveform design in RSN to make radars coexist. In addition, since the radar channel is narrowband, we also consider the bandwidth constraint.

In our RSNs, we choose the CF pulse waveform, which can be defined as

$$x(t) = \sqrt{\frac{E}{T}} \exp(j2\pi\beta t), \qquad -T/2 \leq t \leq T/2 \quad (1)$$

where β is the RF carrier frequency in rad/s. In radar, ambiguity function (AF) is an analytical tool for waveform design and analysis, which succinctly characterizes the behavior of a waveform paired with its matched filter. The AF is useful for examining resolution, side lobe behavior, and ambiguities in both range and Doppler for a given waveform [18]. For a single radar, the matched filter for waveform $x(t)$ is

$x^*(-t)$ and the AF of CF pulse waveform is

$$A(\tau, F_D) = \left| \int_{-T/2+\tau}^{T/2} x(t)\exp(j2\pi F_D s)x^*(t-\tau)dt \right|$$

$$= \left| \frac{E\sin[\pi F_D(T-|\tau|)]}{T\pi F_D} \right|, \qquad -T \leq \tau \leq T. \tag{2}$$

We can simplify this AF in the following three special cases:

1) When $\tau = 0$,

$$A(0, F_D) = \left| \frac{E\sin(\pi F_D T)}{T\pi(F_D)} \right|. \tag{3}$$

2) When $F_D = 0$,

$$A(\tau, 0) = \left| \frac{E(T-|\tau|)}{T} \right|. \tag{4}$$

3) When $\tau = F_D = 0$,

$$A(0,0) = E. \tag{5}$$

Note that the above ambiguity is for one radar only (no coexisting radar).

For RSNs the waveforms from different radars interfere with each other. We choose the waveform for radar i as

$$x_i(t) = \sqrt{\frac{E}{T}}\exp[j2\pi(\beta + \delta_i)t], \qquad -T/2 \leq t \leq T/2 \tag{6}$$

which means that there is a frequency shift δ_i for radar i. To minimize the interference from one waveform to another, optimal values for δ_i should be determined to make the waveforms orthogonal to each other, i.e., let the cross-correlation between $x_i(t)$ and $x_n(t)$ be 0,

$$\int_{-T/2}^{T/2} x_i(t)x_n^*(t)dt$$

$$= \frac{E}{T}\int_{-T/2}^{T/2}\exp[j2\pi(\beta + \delta_i)t]\exp[-j2\pi(\beta + \delta_n)t]dt \tag{7}$$

$$= E\,\mathrm{sinc}[\pi(\delta_i - \delta_n)T]. \tag{8}$$

If we choose

$$\delta_i = \frac{i}{T} \tag{9}$$

where i is a dummy index, (8) can be written as

$$\int_{-T/2}^{T/2} x_i(t)x_n^*(t)dt = \begin{cases} E & i = n \\ 0 & i \neq n \end{cases}. \tag{10}$$

Therefore choosing $\delta_i = i/T$ in (6) yields orthogonal waveforms, i.e., the waveforms can coexist if the carrier spacing is a multiple of $1/T$ between two radar waveforms. In other words, orthogonality amongst

carriers can be achieved by separating the carriers by a multiple of the inverse of waveform pulse duration. With this design, all the orthogonal waveforms can work simultaneously. However, there may exist time-delay and Doppler-shift ambiguity which may interfere with other waveforms in RSN.

III. INTERFERENCES OF WAVEFORMS IN RADAR SENSOR NETWORKS

A. RSN with Two Radar Sensors

We are interested in analyzing the interference from one radar to another if a time delay and Doppler shift are present. For a simple case where there are two radar sensors (i and n), the AF of radar i (considering the interference from radar n) is

$$A_i(t_i, t_n, F_{D_i}, F_{D_n})$$

$$= \left| \int_{-\infty}^{\infty} [x_i(t)\exp(j2\pi F_{D_i}t) + x_n(t-t_n)\right.$$

$$\left. \times \exp(j2\pi F_{D_n}t)]x_i^*(t-t_i)dt \right| \tag{11}$$

$$\leq \left| \int_{-T/2+\max(t_i,t_n)}^{T/2+\min(t_i,t_n)} x_n(t-t_n)\exp(j2\pi F_{D_n}t)x_i^*(t-t_i)dt \right|$$

$$+ \left| \int_{-T/2+t_i}^{T/2} x_i(t)\exp(j2\pi F_{D_i}t)x_i^*(t-t_i)dt \right| \tag{12}$$

$$= \left| \int_{-T/2+\max(t_i,t_n)}^{T/2+\min(t_i,t_n)} x_n(t-t_n)\exp(j2\pi F_{D_n}t)x_i^*(t-t_i)dt \right|$$

$$+ \left| \frac{E\sin[\pi F_{D_i}(T-|t_i|)]}{T\pi F_{D_i}} \right|. \tag{13}$$

To make the analysis easier, it is generally assumed that the radar sensor platform has access to the Global Positioning System (GPS) and the inertial navigation unit (INU) timing and navigation data [3]. In this paper, we assume that the radar sensors are synchronized and that $t_i = t_n = \tau$. Then (13) can be simplified as

$$A_i(\tau, F_{D_i}, F_{D_n}) \approx |E\,\mathrm{sinc}[\pi(n-i+F_{D_n}T)]|$$

$$+ \left| \frac{E\sin[\pi F_{D_i}(T-|\tau|)]}{T\pi F_{D_i}} \right|. \tag{14}$$

We have the following three special cases:

1) If $F_{D_i} = F_{D_n} = 0$, and δ_i and δ_n follow (9), (14) becomes

$$A_i(\tau, 0, 0) \approx \left| \frac{E(T-|\tau|)}{T} \right|. \tag{15}$$

2) If $\tau = 0$, (14) becomes

$$A_i(0, F_{D_i}, F_{D_n}) \approx |E\,\mathrm{sinc}[\pi(n-i+F_{D_n}T)]|$$

$$+ \left| \frac{E\sin(\pi F_{D_i}T)}{T\pi F_{D_i}} \right|. \tag{16}$$

3) If $F_{D_i} = F_{D_n} = 0$, $\tau = 0$, and δ_i and δ_n follow (9), (14) becomes

$$A_i(0,0,0) \approx E. \qquad (17)$$

B. RSN with M Radar Sensors

Our analysis on an RSN with two radar sensors can be extended to the case of M radars. Assuming that the time delay τ for each radar is the same, then the AF of radar 1 (considering interferences from all the other $M-1$ radars with CF pulse waveforms) can be expressed as

$$A_1(\tau, F_{D_1}, \ldots, F_{D_M}) \approx \sum_{i=2}^{M} |E \operatorname{sinc}[\pi(i-1+F_{D_i}T)]|$$
$$+ \left| \frac{E \sin[\pi F_{D_1}(T-|\tau|)]}{T\pi F_{D_1}} \right|. \qquad (18)$$

Similarly, we have the following three special cases:

1) $F_{D_1} = F_{D_2} = \cdots = F_{D_M} = 0$ and the frequency shift δ_i in (6) for each radar follows (9); then (18) becomes

$$A_1(\tau,0,0,\ldots,0) \approx \left| \frac{E(T-|\tau|)]}{T} \right|. \qquad (19)$$

Comparing it against (4), we notice that a radar may exist that can get the same signal strength as that of the single radar in a single radar system (no coexisting radar) when the Doppler shift is 0.

2) If $\tau = 0$, then (18) becomes

$$A_1(0, F_{D_1}, F_{D_2}, \ldots, F_{D_M}) \approx \sum_{i=2}^{M} |E \operatorname{sinc}[\pi(i-1+F_{D_i}T)]|$$
$$+ \left| \frac{E \sin(\pi F_{D_1}T)}{T\pi F_{D_1}} \right|. \qquad (20)$$

Compared with (3), a radar in RSN has higher interferences when unknown Doppler shifts exist.

3) $F_{D_1} = F_{D_2} = \cdots = F_{D_M} = 0$, $\tau = 0$ and δ_i in (6) follows (9); then (18) becomes

$$A_1(0,0,0,\ldots,0) \approx E. \qquad (21)$$

IV. NEW FOR COLLABORATIVE AUTOMATIC TARGET RECOGNITION

In NEW, the radar sensors are networked together in an ad hoc fashion. They do not rely on a preexisting fixed infrastructure, such as a wireless backbone network or a base station. They are self-organizing entities that are deployed on demand in support of various events, surveillance, battlefield, disaster relief, search and rescue, etc. Scalability concern suggests a hierarchical organization of radar sensor networks with the lowest level in the hierarchy being a cluster. As argued in [9, 10, 13, 17], in
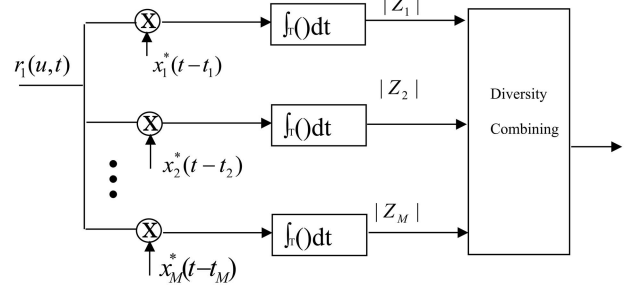
Fig. 1. Waveform diversity combining by clusterhead in RSN.

addition to helping with scalability and robustness, aggregating sensor nodes into clusters has additional benefits:

1) conserving radio resources such as bandwidth,
2) promoting spatial code reuse and frequency reuse,
3) simplifying the topology, e.g., when a mobile radar changes its location, it is sufficient for the nodes in the attended clusters to update their topology information,
4) reducing the generation and propagation of routing information, and
5) concealing the details of global network topology from individual nodes.

In RSN, each radar can provide its waveform parameters such as δ_i to its clusterhead radar, and the clusterhead radar can combine the waveforms from its cluster members.

In RSN with M radars, the received signal for clusterhead (assume it's radar 1) is

$$r_1(u,t) = \sum_{i=1}^{M} \alpha(u)x_i(t-t_i)\exp(j2\pi F_{D_i}t) + n(u,t)$$
$$(22)$$

where $\alpha(u)$ stands for radar cross section (RCS), which can be modeled using non-zero constants for nonfluctuating targets and four Swerling target models for fluctuating targets [18]; F_{D_i} is the Doppler shift of the target relative to waveform i; t_i is the delay of waveform i; and $n(u,t)$ is the additive white Gaussian noise (AWGN). In this paper, we propose a RAKE structure for waveform diversity combining, as illustrated by Fig. 1. The RAKE structure is so named because it reminds one of a garden rake, each branch collecting echo energy in a way similar to how tines on a rake collect leaves. This figure summarizes how the clusterhead works. The received signal $r_1(u,t)$ consists of echoes triggered by the waveforms from each radar sensor, $x_i^*(t-t_i)$ is used to retrieve the amplified waveform from radar i (amplified by the target RCS) based on the orthogonal property presented in Sections II and III, and then this information is time-averaged for diversity combining.

According to this structure, the received $r_1(u,t)$ is processed by a bank of matched filters, then the output of branch 1 (after integration) is

$$Z_1(u;t_1,\ldots,t_M,F_{D_1},\ldots,F_{D_M})$$

$$= \int_{-T/2}^{T/2} r_1(u,t)x_1^*(t-t_1)ds \qquad (23)$$

$$= \int_{-T/2}^{T/2} \left[\sum_{i=1}^{M} \alpha_i(u)x_i(t-t_i)\exp(j2\pi F_{D_i}t) + n(u,t) \right]$$

$$\times x_1^*(t-t_1)dt. \qquad (24)$$

Assuming $t_1 = t_2 = \cdots = t_M = \tau$, then based on (18),

$$Z_1(u;\tau,F_{D_1},\ldots,F_{D_M}) \approx \sum_{i=2}^{M} \alpha(u)E\,\text{sinc}[\pi(i-1+F_{D_i}T)]$$

$$+ \frac{\alpha(u)E\sin[\pi F_{D_1}(T-|\tau|)]}{T\pi F_{D_1}} + n(u,\tau). \qquad (25)$$

Similarly, we can get the output for any branch m ($m = 1,2,\ldots,M$);

$$Z_m(u;\tau,F_{D_1},\ldots,F_{D_M}) \approx \sum_{i=1,i\neq m}^{M} \alpha(u)E\,\text{sinc}[\pi(i-m+F_{D_i}T)]$$

$$+ \frac{\alpha(u)E\sin[\pi F_{D_m}(T-|\tau|)]}{T\pi F_{D_m}} + n(u,\tau). \qquad (26)$$

Therefore $Z_m(u;\tau,F_{D_1},\ldots,F_{D_M})$ consists of three parts, namely, signal (reflected signal from radar m waveform) $\alpha(u)E\sin[\pi F_{D_m}(T-|\tau|)]/T\pi F_{D_m}$, interferences from other waveforms $\sum_{i=1,i\neq m}^{M} \alpha(u) \cdot E\,\text{sinc}[\pi(i-m+F_{D_i}T)]$, and noise $n(u,\tau)$.

We can also have the following three special cases for $|Z_m(u;\tau,F_{D_1},\ldots,F_{D_M})|$:

1) When $F_{D_1} = \cdots = F_{D_M} = 0$,

$$Z_m(u;\tau,0,0,\ldots,0) \approx \frac{E\alpha(u)(T-|\tau|)}{T} + n(u,\tau) \qquad (27)$$

which means that if there is no Doppler mismatch, there is no interference from other waveforms.

2) If $\tau = 0$, (26) becomes

$$Z_m(u;0,F_{D_1},\ldots,F_{D_M})$$

$$\approx \sum_{i=1,i\neq m}^{M} \alpha(u)E\,\text{sinc}[\pi(i-m+F_{D_i}T)]$$

$$+ \frac{\alpha(u)E\sin[\pi F_{D_m}T]}{T\pi F_{D_m}} + n(u). \qquad (28)$$

3) If $\tau = 0$, and $F_{D_1} = \cdots = F_{D_M} = 0$, (26) becomes

$$Z_m(u;0,0,0,\ldots,0) \approx E\alpha(u) + n(u). \qquad (29)$$

Doppler mismatch happens quite often in a target search where the target velocity is not yet known. However, in target recognition, generally high-resolution measurements of targets in range ($\tau = 0$) and Doppler are available; therefore, (29) will be used for CATR.

The process of combining all the Z_ms ($m = 1,2,\ldots,M$) is very similar to the diversity combining in wireless communications that combats channel fading, and the combination schemes may be different for different applications. In this paper, we are interested in applying the RSN waveform diversity to CATR, e.g., recognizing that the echo on a radar display is that of an aircraft, ship, motor vehicle, bird, person, rain, chaff, clear-air turbulence, land clutter, sea clutter, bare mountains, forested areas, meteors, aurora, ionized media, or other natural phenomena via collaborations among different radars. Early radars were "blob" detectors in that they detected the presence of a target and gave its location in range and angle; then, radar began to be more than a blob detector and could provide recognition of one type of target from another [21]. It is known that small changes in the aspect angle of complex (multiple scatter) targets can cause major changes in the RCS. This has been considered in the past as a means of target recognition, and is called RCS, but it has not had much success [21]. In [19], a parametric filtering approach was proposed for target detection using airborne radar. In [14], knowledge-based sensor networks were applied to threat assessment. In this paper, we propose ML-CATR algorithms for nonfluctuating targets as well as fluctuating targets.

A. ML-CATR for Nonfluctuating Targets

In some sources, the nonfluctuating target is identified as a "Swerling 0" or "Swerling 5" model [22]. For nonfluctuating targets, the RCS $\alpha_m(u)$ is just a constant α for a given target. In (29), $n(u,\tau)$ is a zero-mean Gaussian random variable for a given τ, so $|Z_m(u;0,0,\ldots,0)|$ follows a Rician distribution because signal $E\alpha(u)$ is a positive constant, $E\alpha$, for a nonfluctuating target. Let $y_m \overset{\Delta}{=} |Z_m(u;0,0,\ldots,0)|$; then the probability density function (pdf) of y_m is

$$f(y_m) = \frac{2y_m}{\sigma^2}\exp\left[-\frac{(y_m^2+\lambda^2)}{\sigma^2}\right]I_0\left(\frac{2\lambda y_m}{\sigma^2}\right) \qquad (30)$$

where

$$\lambda = E\alpha \qquad (31)$$

σ^2 is the noise power (with I and Q subchannel power $\sigma^2/2$), and $I_0(\cdot)$ is the zero-order modified Bessel function of the first kind. Let $\mathbf{y} \overset{\Delta}{=} [y_1,y_2,\ldots,y_M]$; then the pdf of $\mathbf{y}$ is

$$f(\mathbf{y}) = \prod_{m=1}^{M} f(y_m). \qquad (32)$$

Our CATR is a multiple-category hypothesis testing problem, i.e., it decides a target category (e.g., aircraft, ship, motor vehicle, bird, etc.) based on $r_1(u,t)$. Assume there are a total of N categories, and a category n target has RCS α_n; therefore the ML-CATR algorithm to decide a target category C can be expressed as

$$C = \arg\max_{n=1}^{N} f(\mathbf{y} \mid \lambda = E\alpha_n) \qquad (33)$$

$$= \arg\max_{n=1}^{N} \prod_{m=1}^{M} \frac{2y_m}{\sigma^2} \exp\left[-\frac{(y_m^2 + E^2\alpha_n^2)}{\sigma^2}\right] I_0\left(\frac{2E\alpha_n y_m}{\sigma^2}\right). \qquad (34)$$

B. ML-CATR for Fluctuating Targets

Fluctuating target modeling is more realistic when the target RCS is drawn from either the Rayleigh or chi-square of a deg four pdf. The Rayleigh model describes the behavior of a complex target consisting of many scatters, none of which is dominant. The fourth-degree chi-square model targets have many scatters of similar strength with one dominant scatter. Based on different combinations of pdf and decorrelation characteristics (scan-to-scan or pulse-to-pulse decorrelation), four Swerling models are used [18]. In this paper we focus on the "Swerling 2" model, which is a Rayleigh distribution with pulse-to-pulse decorrelation. The pulse-to-pulse decorrelation implies that each individual pulse results in an independent value for RCS α.

For the Swerling 2 model, the RCS $|\alpha(u)|$ follows a Rayleigh distribution, and its I and Q subchannels follow zero-mean Gaussian distributions with a variance γ^2. Assume

$$\alpha(u) = \alpha_I(u) + j\alpha_Q(u) \qquad (35)$$

and $n(u) = n_I(u) + jn_Q(u)$ follows a zero-mean complex Gaussian distribution with a variance σ^2 for the I and Q subchannels. Therefore, according to (29), $Z_m(u;0,0,0,\ldots,0)$ is a zero-mean Gaussian random variable with a variance $E^2\gamma^2 + \sigma^2$ for the I and Q subchannels, which means $y_m \overset{\Delta}{=} |Z_m(u;0,0,\ldots,0)|$ follows a Rayleigh distribution with a parameter $\sqrt{E^2\gamma^2 + \sigma^2}$:

$$f(y_m) = \frac{y_m}{E^2\gamma^2 + \sigma^2} \exp\left(-\frac{y_m^2}{E^2\gamma^2 + \sigma^2}\right). \qquad (36)$$

The mean value of y_m is $\sqrt{\pi(E^2\gamma^2 + \sigma^2)/2}$, and the variance is $(4-\pi)(E^2\gamma^2 + \sigma^2)/2$. The variance of signal is $(4-\pi)E^2\gamma^2/2$, and the variance of noise is $(4-\pi)\sigma^2/2$.

Let $\mathbf{y} \overset{\Delta}{=} [y_1, y_2, \ldots, y_M]$; then the pdf of $\mathbf{y}$ is

$$f(\mathbf{y}) = \prod_{m=1}^{M} f(y_m). \qquad (37)$$

Assume there are a total of N categories, and a category n target has a RCS $\alpha_n(u)$ (with a variance γ_n^2), so the ML-ATR algorithm to decide a target category C can be expressed as

$$C = \arg\max_{n=1}^{N} f(\mathbf{y} \mid \gamma = \gamma_n) \qquad (38)$$

$$= \arg\max_{n=1}^{N} \prod_{m=1}^{M} \frac{y_m}{E^2\gamma_n^2 + \sigma^2} \exp\left(-\frac{y_m^2}{E^2\gamma_n^2 + \sigma^2}\right). \qquad (39)$$

V. SIMULATIONS AND REAL-WORLD APPLICATION EXAMPLE

A. Computer Simulations

RSNs will be required to detect a broad range of target classes. Too often, the characteristics of objects that are not of interest (e.g., bird) are similar to those of threat objects (e.g., missile). Therefore, new techniques to distinguish threats from undesired detections (e.g., birds, etc.) are needed. We applied our ML-CATR to this important application to recognize a target from many target classes. We assume that the domain of target classes is known a priori (N in Sections IVA and IVB), and that the RSN is confined to work only on the known domain.

For nonfluctuating target recognition, our targets have 5 classes with different RCS values, which are summarized in Table I [21]. We applied the ML-CATR algorithms in Section IVA (for the nonfluctuating target case) to classify an unknown target as one of these 5 target classes. At each average signal-to-noise ratio (SNR) value, we ran Monte-Carlo simulations for 10^5 times for each target. The average SNR value is based on the average power from all targets (signal variance), so the actual SNRs for bird and missile are much lower than the average SNR value, for example, at the average SNR = 16 dB, the bird target SNR = −33.1646 dB, and the missile target SNR = 0.8149 dB; and at average SNR = 20 dB, the bird target SNR = −29.1646 dB, and the missile target SNR = 4.8149 dB. In Figs. 2(a), 2(b), we plotted the probability of the automatic target recognition (ATR) error in bird and missile recognition when they are assumed to be nonfluctuating targets. These figures indicate that a single radar system can't perform well in both recognitions, because the probability of the ATR error is above 10%, which cannot be used for real-world ATR. However, the 5-radar RSN and 10-radar RSN can maintain very low ATR errors. In Fig. 2(c), we plotted the average probability of the ATR error for all 5 targets. Since the other 3 targets (different aircrafts) have much higher SNRs, their ATR error is lower, which makes the average probability of ATR error lower.

TABLE I
RCS Values at Microwave Frequency for 5 Targets

Index n	Target	RCS
1	Bird	0.01
2	Conventional unmanned winged missile	0.5
3	Small single-engine aircraft	1
4	Small fighter aircraft or 4 passenger jet	2
5	Large fighter aircraft	6

For fluctuating target recognition, we assume the fluctuating targets follow the Swerling 2 model (Rayleigh distribution with pulse-to-pulse decorrelation), and assume the RCS value listed in Table I to be the standard deviation (std) γ_n of RCS $\alpha_n(u)$ for target n. We applied the ML-CATR algorithm in Section IVB (for the fluctuating target case) for target recognition within the 5-targets domain. Similarly we ran Monte-Carlo simulations at each SNR value. In Figs. 3(a), 3(b), 3(c), we plotted the ATR performance for fluctuating targets and compared the performances of a single-radar system, a 5-radar RSN, and a 10-radar RSN. Observe that the two RSNs perform much better than the single-radar system. The ATR error for the missile is higher than that for the bird because the Rayleigh distribution of the missile has a lot of overlap with its neighbor targets (aircrafts). Comparing Figs. 2(a), 2(b), 2(c) to Figs. 3(a), 3(b), 3(c), it is clear that higher SNRs are needed for the fluctuating target recognition as compared with the nonfluctuating target recognition. According to Skolnik [21], the radar performance with a probability of recognition error (p_e) less than 10% is good enough. Our RSN with waveform-diversity can achieve a probability of ATR error much less than 10% for each target ATR as well as the average ATR for all targets. However, the single-radar system has a probability of ATR error much higher than 10%. Fig. 3(c) also tells us that it is impossible for the average probability of ATR error of a single-radar system to be less than 10%, even at an extremely high SNR. Our RSN with waveform diversity is very promising for real-world ATR.

B. Real-World Application Example

We verified our approach based on a real-world application example, sense-through-foliage target detection from the U.S. Air Force Research Laboratory. The target is a trihedral reflector (as shown in Fig. 4) in a forest. We plot two collections using ultra wideband (UWB) radars in Figs. 5(a) and 5(b). Fig. 5(a) has no target in range, and Fig. 5(b) has a target at samples around 13,900. We plot the echo differences between Figs. 5(a) and 5(b) in Fig. 5(c). However, it is impossible to identify whether there is any target or where that target is, based on Fig. 5(c), which means single radar
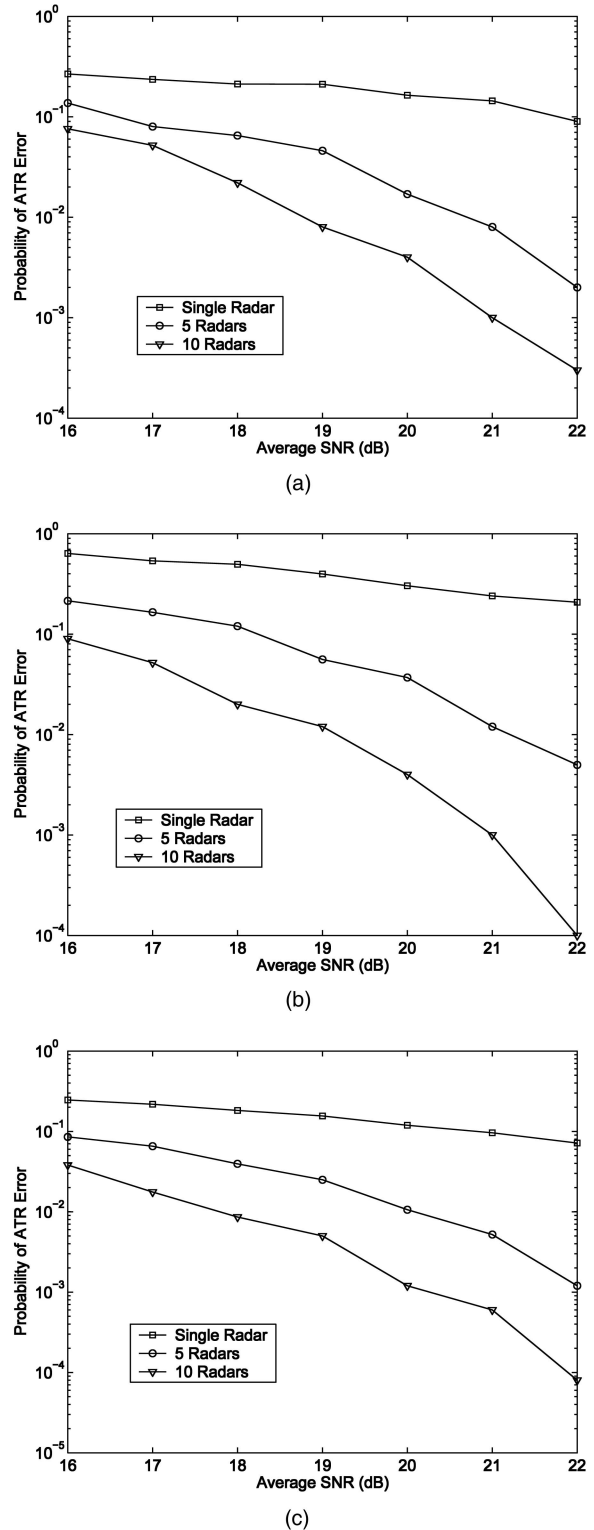
Fig. 2. Probability of ATR error for nonfluctuating targets at different average SNR (dB) values. (a) Bird. (b) Missile. (c) Average probability of ATR error for 5 targets.

doesn't work even in the ideal case. Since significant pulse-to-pulse variability exists in the echoes, this motivates us to explore the spatial and time diversity using the radar sensor networks approach. The echoes, i.e., RF responses by the pulse of each cluster-member
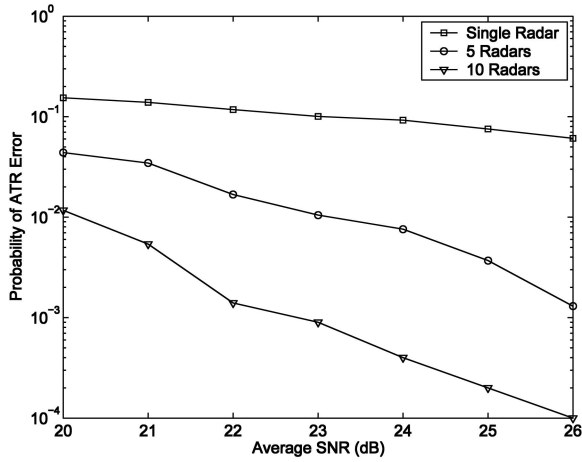
(a)
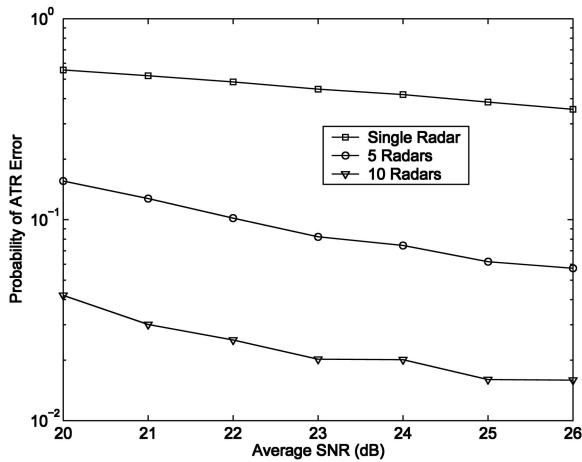
(b)
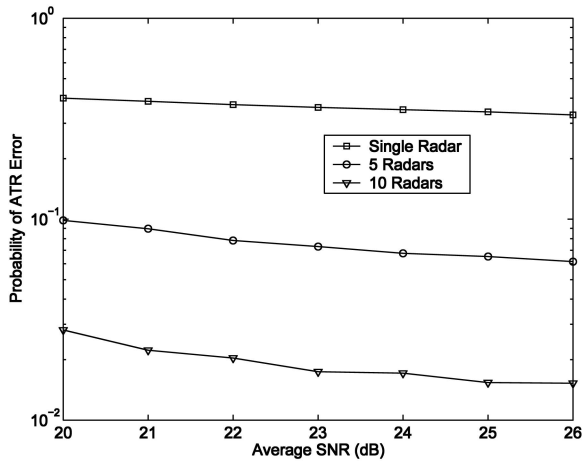
(c)

Fig. 3. Probability of ATR error for fluctuating targets at different average SNR (dB) values. (a) Bird. (b) Missile. (c) Average probability of ATR error for 5 targets.

Fig. 4. Target (a trihedral reflector) shown on stand at 300 ft from measurement lift.

without target, respectively). Observe that in Fig. 6(b), the power of ac values (around sample 13,900) where the target is located is nonfluctuating (monotonically increasing, then decreasing). Although some other samples also have very high ac power values, it is very clear that they are fluctuating, and the power of ac values behaves like random noise because, generally, the clutter has Gaussian distribution in the frequency domain.

VI. CONCLUSIONS AND FUTURE WORKS

We have studied the CF pulse waveform design and diversity in RSNs. We showed that the waveforms can coexist if the carrier frequency spacing is a multiple of $1/T$ between two radar waveforms. We made analysis on interferences among waveforms in RSN and proposed a RAKE structure for waveform diversity combining in RSN. As an application example, we applied the waveform design and diversity to CATR in RSN and proposed ML-CATR algorithms for nonfluctuating targets as well as fluctuating targets. Simulation results show that an RSN using our waveform diversity-based ML-ATR algorithms performs much better than a single-radar system for nonfluctuating targets and fluctuating targets recognition. We also validated our RSN approach via a real-world sense-through-foliage target detection example.

In our future research, we will investigate the CATR when multiple targets coexist in RSN and when the number of targets are time varying. In this paper, we used spatial diversity combining. For multitarget ATR, we will further investigate spatial-temporal-frequency combining for waveform diversity in RSN.

radar, are combined by the clusterhead using the RAKE structure in Fig. 1.

We ran simulations for an RSN with 30 radar sensors, and plotted the power of ac values in Figs. 6(a) and 6(b) for the two cases (with target and
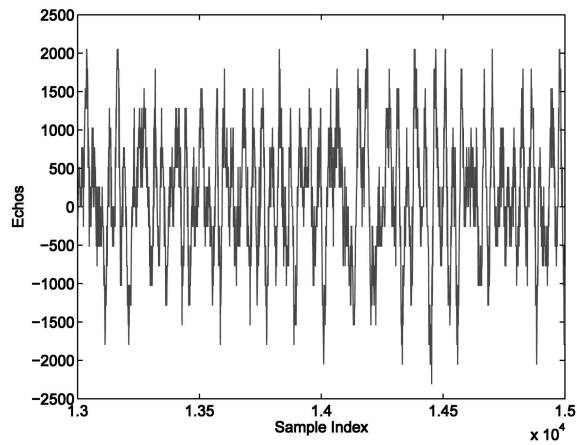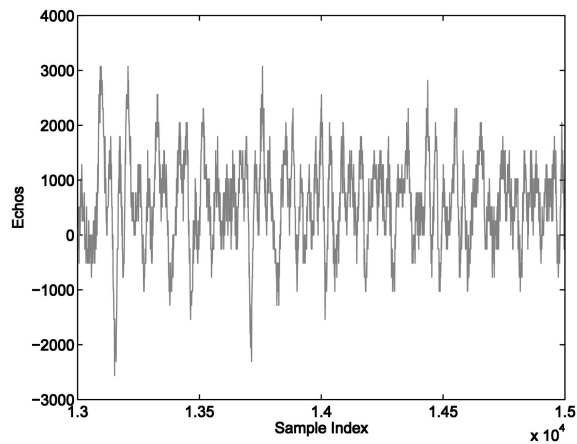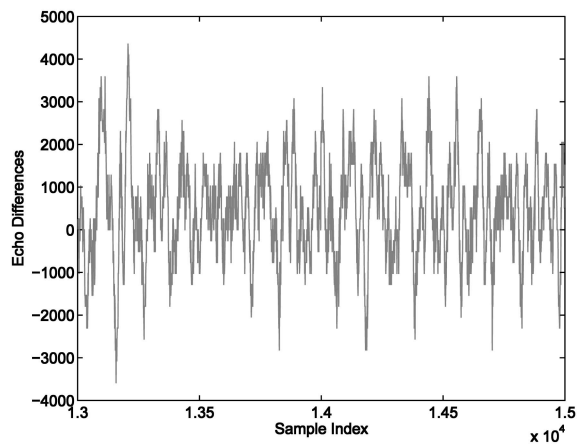
Fig. 5. Measurement of UWB radar. (a) Expanded view of traces (no target) from sample 13,001 to 15,000. (b) Expanded view of traces (with target) from sample 13,001 to 15,000. (c) Differences between (a) and (b).

REFERENCES

[1]   ONR BAA 06-016
         Command and Control and Combat Systems (C2 and CS).
         Online: available http://www.onr.navy.mil/02/baa/ expired.asp.
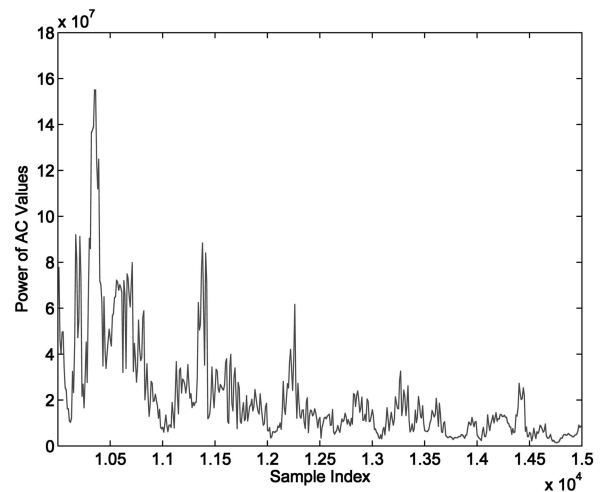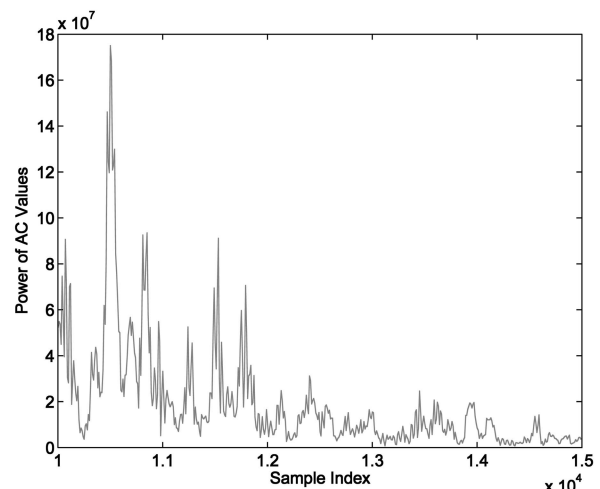
Fig. 6. Power of ac values based on RSNs approach. (a) No target. (b) With target in field (in samples around 13,900).

[2]   ONR BAA 07-009
         Electronic Warfare Discovery and Invention (D&I).
         Online: available http://www.onr.navy.mil/02/baa/.
[3]   ONR BAA 07-017
         NET-SENTRIC Surveillance.
         Online: available http://www.onr.navy.mil/02/baa/.
[4]   Baggenstoss, P.
         Adaptive pulse length correction (APLECORR): A strategy for waveform optimization in ultrawideband active sonar.
         IEEE Transactions on Oceanic Engineering, **23**, 1 (1998), 1–11.
[5]   Baum, C. E., et al.
         The singularity expansion method and its application to target identification.
         Proceedings of the IEEE, **79**, 10 (Oct. 1991).
[6]   Bell, M. R.
         Information theory and radar waveform design.
         IEEE Transactions on Information Theory, **39**, 5 (Sept. 1993), 1578–1597.
[7]   Deng, H.
         Synthesis of binary sequences with good correlation and cross-correlation properties by simulated annealing.
         IEEE Transactions on Aerospace and Electronic Systems, **32**, 1 (Jan. 1996).

[8]   Fitzgerald, R.
       Effects of range-Doppler coupling on chirp radar tracking
       accuracy.
       IEEE Transactions on Aerospace and Electronic Systems,
       10 (July 1974), 528–532.

[9]   Hou, T-C., and Tsai, T-J.
       An access-based clustering protocol for multihop wireless
       ad hoc networks.
       IEEE Journal of Selected Areas in Communications, **19**, 7
       (July 2001), 1201–1210.

[10]   Iwata, A., Chiang, C. C., Pei, G., Gerla, M., and Chen, T. W.
       Scalable routing strategies for ad hoc networks.
       IEEE Journal of Selected Areas in Communications, **17**
       (1999), 1369–1379.

[11]   Johnson, R. A., and Titlebaum, E. L.
       Range Doppler uncoupling in the Doppler tolerant bat
       signal.
       In *Proceedings of IEEE Ultrasonics Symposium*, New
       York, 1972, 64–67.

[12]   Kershaw, D., and Evans, R.
       Optimal waveform selection for tracking system.
       IEEE Transactions on Information Theory, **40**, 5 (1994),
       1536–1550.

[13]   Lin, C. R., and Gerla, M.
       Adaptive clustering in mobile wireless networks.
       IEEE Journal of Selected Areas in Communications, **16**
       (1997), 1265–1275.

[14]   Liang, Q., and Cheng, X.
       KUPS: Knowledge-based ubiquitous and persistent sensor
       networks for threat assessment.
       IEEE Transactions on Aerospace and Electronic Systems,
       44, 3 (July 2008).

[15]   Niu, R., Willett, P., and Bar-Shalom, Y.
       Tracking consideration in selection of radar waveform for
       range and range-rate measurements.
       IEEE Transactions on Aerospace and Electronic Systems,
       38, 2 (2002).

[16]   Papandreou, A., Boudreaux-Bartels, G. F., and Kay, S. M.
       Detection and estimation of generalized chirps using
       time-frequency representation.
       In *Twenty-Eighth Asilomar Conference on Signals, Systems
       and Computers*, vol. 1, Oct. 1994, 50–54.

[17]   Perkins, C. E.
       Cluster-Based Networks.
       In C. E. Perkins (Ed.), *Ad Hoc Networking*, Boston:
       Addison-Wesley, 2001, ch. 4, 75–138.

[18]   Richards, M. A.
       Fundamentals of Radar Signal Processing.
       New York: McGraw-Hill, 2005.

[19]   Roman, J., Rangaswamy, M., Davis, D., Zhang, Q.,
       Himed, B., and Michels, J.
       Parametric adaptive matched filter for airborne radar
       applications.
       IEEE Transactions on Aerospace and Electronic Systems,
       36, 2 (2000), 677–692.

[20]   Sarkar, T. K., and Sangruji, N.
       An adaptive nulling system for a narrow-band signal with
       a look-direction constraint utilizing the conjugate gradient
       method.
       IEEE Transactions on Antennas and Propagation, **37**, 7
       (July 1989), 940–944.

[21]   Skolnik, M. I.
       Introduction to Radar Systems (3rd ed.).
       New York: McGraw-Hill, 2001.

[22]   Swerling, P.
       Probability of detection for fluctuating targets.
       IRE Transactions on Information Theory, **6** (Apr. 1960),
       269–308.

[23]   Sowelam, S., and Tewfik, A.
       Waveform selection in radar target classification.
       IEEE Transactions on Information Theory, **46**, 3 (2000),
       1014–1029.

[24]   Stankovic, L., Thayaparan, T., and Dakovic, M.
       Signal decomposition by using the S-method with
       application to the analysis of HF radar signals in
       sea-clutter.
       IEEE Transactions on Signal Processing, **54**, 11 (Nov.
       2006), 4332–4342.

[25]   Sun, Y., Willett, P., and Lynch, R.
       Waveform fusion in sonar signal processing.
       IEEE Transactions on Aerospace and Electronic Systems,
       40, 2 (2004).

Qilian Liang is an associate professor in the Department of Electrical Engineering, University of Texas at Arlington. He received the B.S. degree from Wuhan University in 1993, M.S. degree from Beijing University of Posts and Telecommunications in 1996, and Ph.D. from University of Southern California (USC) in May 2000, all in electrical engineering.

Prior to joining the faculty of the University of Texas at Arlington in August 2002, he was a member of the technical staff in Hughes Network Systems, Inc. in San Diego, CA. His research interests include radar sensor networks, wireless sensor networks, wireless communications, communication system and communication theory, signal processing for communications, fuzzy logic systems and applications, collaborative and distributed signal processing, etc.

Dr. Liang has published more than 160 journal and conference papers, 7 book chapters, and has 6 U.S. patents pending. He received the 2002 IEEE Transactions on Fuzzy Systems Outstanding Paper Award, 2003 U.S. Office of Naval Research (ONR) Young Investigator Award, 2005 UTA College of Engineering Outstanding Young Faculty Award, and 2007 U.S. Air Force Summer Faculty Fellowship Program Award.

Xiuzhen (Susan) Cheng is an associate professor in the Department of Computer Science, The George Washington University. She received her M.S. degree and Ph.D. in computer science from the University of Minnesota, Twin Cities in 2000 and 2002, respectively.
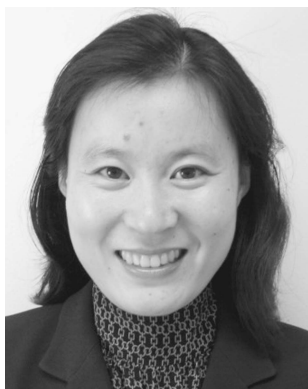
Her current research interests include wireless and mobile computing, sensor networking, wireless and mobile security, and algorithm design and analysis.

Dr. Cheng has served on the editorial boards of several technical journals and in the technical program committees of various professional conferences/workshops. She is a program cochair or vice cochair for several conferences such as WASA'06, ICPP'09, and MASS'09. Dr. Cheng worked as a program director in the National Science Foundation (NSF) for 6 months in 2006 and joined NSF again as a part-time program director in April 2008. She received the NSF CAREER Award in 2004.

Sherwood W. Samn was born in Los Angeles, CA, in 1941. He received his B.A. degree in physics and mathematics and Ph.D. in applied mathematics from the University of California, Berkeley, in 1963 and 1968, respectively.
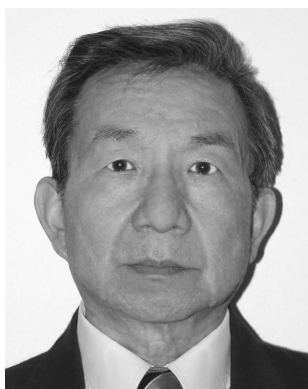
From 1968 to 1974 he taught at the Indiana University–Purdue University at Indianapolis. Since then he has joined the Mathematics Group at the Air Force Research Laboratory at Brooks City-Base in San Antonio, TX. He has published in functional analysis, optimal control, statistics, operations research, integral equations, and FDTD modeling. His current interests are electromagnetic propagation, signal processing, and antenna design with emphasis on their applications to detection problems.